Structural and bonding properties of solid tellurium from first-principles calculations

Florian Kirchhoff,* Nadia Binggeli, and Giulia Galli
Institut Romand de Recherche Numérique en Physique des Matériaux, IN-Ecublens, 1015 Lausanne, Switzerland

Sandro Massidda
Dipartimento di Scienze Fisiche, Università degli Studi di Cagliari, 09124 Cagliari, Italy
(Received 17 May 1994)

We have studied the structural and bonding properties of the equilibrium and high-pressure phases of tellurium by means of first-principles total-energy calculations, performed within the local-density approximation. The calculated characteristics of the various polymorphs under pressure show good general agreement with existing experiments. However, some systematic discrepancies occur between computed and measured structural parameters for the open linear-chain (trigonal) and layer-type (orthorhombic) phases. The interchain and interlayer distances are underestimated within the local-density approach, and the relative stability of the trigonal and of the orthorhombic phase with respect to compact metallic structures is lower in the calculations than indicated by the experimental phase diagram. The complex structural changes of Te under pressure are discussed in terms of the trends under pressure of the different types of bonds involved in the various crystal structures.

I. INTRODUCTION

Recently there has been a growing interest in the study of materials under high-pressure conditions, motivated by the need of synthesizing new solids with targeted physical properties,[1] and animated by the availability of improved experimental techniques.[2] In this context, renewed attention has been given to the group-VIa elements S, Se, and Te, which exhibit very interesting properties under pressure. They undergo complex structural changes, they show semiconductor-to-metal transitions, and some of their high-pressure phases are superconducting at low temperatures.[3–6] Furthermore, an experimental effort has been recently undertaken[7,8] to investigate alloys of S, Se, and Te in both the solid and the liquid phase.

As far as theoretical investigations are concerned, first-principles total-energy calculations have been successfully used to study various properties under pressure of group-IVa elements, such as C,[9] Si,[10] and Sn,[11,12] and of some of their compounds or alloys, e.g., SiO_2,[13] C-N,[14] and GeSe.[15] However, no *ab initio* investigation of the high-pressure properties of more complex open-type structures, such as those of VIa elements, has yet been carried out.

In this paper we present a systematic study of the structural and electronic properties of the high-pressure phases of solid tellurium, in particular of four phases (Te-I,III,IV,V) known in the pressure range 0–40 GPa. Theoretical investigations of tellurium have so far been limited to band structure calculations,[16–19] and most of them have been performed for the trigonal phase (Te-I).[18,19] Some early studies included computations for the rhombohedral (Te-IV) and for the hypothetical simple cubic structure.[20,21] However, these calculations were not performed self-consistently. The only self-consistent calculation for a high-pressure structure was done for the monoclinic phase (Te-II), by using an orthorhombic approximation to the monoclinic unit cell, and by using a local pseudopotential.[22] In all of the theoretical studies that have appeared so far in the literature, the experimental lattice parameters were used as input for the calculations; neither the unit cell nor the internal parameters were relaxed. To our knowledge, total-energy calculations allowing for lattice relaxations have been reported only for the trigonal phase of selenium.[23,24]

In our work, we investigated the structural stability of various Te polymorphs by means of pseudopotential and all-electron first-principles calculations. The different crystal structures were fully optimized in order to compute total energies and pressures as a function of volume. Our results allow a thorough characterization of the complex changes under pressure of the different types of bonds in the various Te structures. Furthermore, they allow a discussion of the relative merits of the local-density approximation in describing bonds with different characteristics, such as metallic, covalent, and so-called weak bonds.

The rest of the paper is organized as follows: In Secs. II we describe the computational method used in our calculations; Secs. III and IV A–IV D contain a discussion of our results for the phase diagram and the structural properties of Te-I, Te-III, Te-IV, and Te-V, respectively. Finally, our conclusion are presented in Sec. V.

II. COMPUTATIONAL METHODS

The calculations were performed within the local-density approximation (LDA) to density functional theory. We employed the plane-wave (PW) pseudopotential method[25] and, in selected cases, the full-potential linearized augmented-plane-wave (FLAPW) method.[26] Within the pseudopotential method we used the exchange-correlation potential of Ceperley and Alder[27] as parametrized by Perdew and Zunger,[28] while in the FLAPW calculations the Hedin-Lundqvist functional[29] was used.

The pseudopotential calculations were carried out with norm-conserving pseudopotentials.[30] The one-electron Schrödinger equations were solved by iterative diagonalization techniques, and by using the Broyden mixing scheme[31] to accelerate self-consistency. Plane waves up to an energy cutoff ($E_{\rm cut}$) of 16 Ry were included in the basis set. Increasing the energy cutoff to 36 Ry altered the energy differences between the various phases by less than 0.02 eV/atom.

The Brillouin zone (BZ) integrations for the semiconducting trigonal phase were performed with the k-point mesh[32] ($4 \times 4 \times 4$) with displacement (0,0,1/4) in reciprocal lattice units. This mesh yields 10 k points in the irreducible part of the BZ. The integrations for the other (metallic) phases were carried out with the Monkhorst-Pack meshes[33] ($10 \times 10 \times 10$), for the simple cubic (sc), rhombohedral, and body-centered-cubic (bcc) structures, and ($8 \times 6 \times 6$) for the orthorhombic structure. These meshes are equivalent to 35, 110, 44, and 72 special k points in the sc, rhombohedral, bcc, and orthorhombic BZ, respectively. As far as the k-point sampling is concerned, we estimated the energies per atom to be converged within a few tenths of mRy. In order to deal with the Fermi surface, we used the Gaussian broadening technique,[34] with a broadening of 0.01 Ry for all phases.

In our PW pseudopotential calculations, forces acting on ionic cores were incorporated in a gradient method[35] to minimize the total energy with respect to the internal parameters. For each phase, and at a given volume, all structural parameters were fully relaxed. This represents a challenge for a phase such as, e.g., the orthorhombic Te-III, which has a complex structure and is metallic. In addition to the extensive k-point sampling needed because of the Fermi surface, the Te-III structure has two cell-shape ratios (b/a, c/a) and six internal parameters that have to be optimized at each volume.

In the FLAPW calculations, the core states were treated self-consistently and fully relativistically, whereas the valence states were treated semirelativistically. Inside the atomic spheres, angular momenta up to $l = 8$ were included in the expansion of the wave functions, charge density, and potential. In the interstitial region the wave functions included plane waves with wave vector $|\mathbf{k} + \mathbf{G}| \leq 2.7$ a.u. corresponding to $E_{\rm cut} \approx 15$ Ry. The Te atomic-sphere radius was taken to be 2.6 a.u. For the high-pressure body-centered-cubic structure, we also investigated whether the treatment of the Te $4d$ states had a significant effect on the structural properties by considering these states among the valence states, in a separate energy window. The FLAPW calculations were performed by using the same k-point meshes as in the pseudopotential calculations for all structures but the bcc, for which we used up to 120 inequivalent k points with the tetrahedron method[36] for the BZ integrations.

III. PHASE DIAGRAM: STRUCTURAL PROPERTIES

In the solid state, five phases of tellurium (Te-I to Te-V) are known in the pressure range 0–40 GPa.[3,17,37] We performed first-principles calculations for all of these phases except for the monoclinic structure, Te-II, which is almost identical to the orthorhombic structure of Te-III. In Figs. 1 and 2 we show the atomic arrangements of Te-I and Te-III, respectively.

Te-I (Fig. 1), which is found experimentally to be the most stable form of tellurium, has three atoms per unit cell. It is characterized by infinite helical chains, with three atoms per turn, parallel to the c axis. As indicated in Fig. 1, the trigonal structure reduces to a simple cubic (sc) one (the α-Po structure) for given values of the internal parameter (u=1/3) and cell-shape ratio (c/a=$\sqrt{3/2}$). The sc structure has also been considered in our study of the relative stability of the various polymorphs.

The structure of Te-III is shown in Fig. 2. It consists of puckered layers parallel to the x-z plane. The layers are stacked along the y direction, and each of them is alternatively shifted by half a lattice constant along the x axis. In Fig. 2 it is also indicated how the rhombohedral structure of Te-IV can be obtained as a special case of the orthorhombic structure of Te-III when the intra- and interlayer distances become equal.

In order to study the relative stability and the pres-

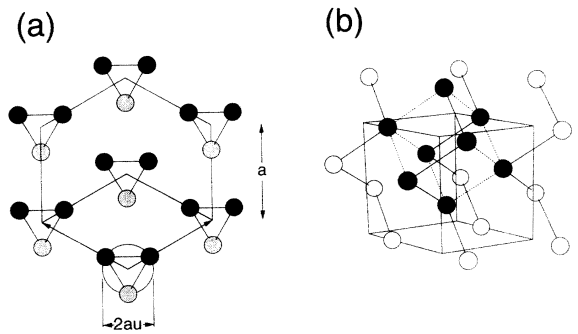

FIG. 1. Crystalline structure of the equilibrium Te-I trigonal phase. Projection of the structure along the c axis (a) and side view (b). The structure is characterized by infinite helical chains with three atoms per turn. The chains are arranged on an hexagonal lattice and are parallel to the c axis. The internal parameter u defines the position of the atoms in the unit cell as $(u,0,0),(0,u,1/3),(\bar{u},\bar{u},2/3)$ in units of the lattice vectors. The radius of the chains is given by au and the interchain distance is $a(1-u)$. The simple cubic structure is a special case of the trigonal structure obtained for $u = 1/3$ and $c/a = \sqrt{3/2}$. The cubic framework is indicated by dashed lines.

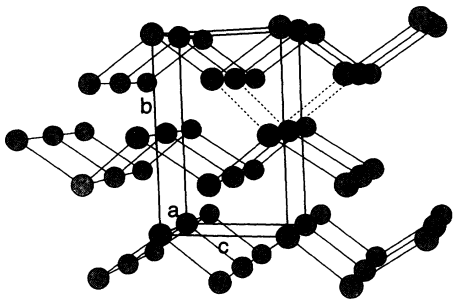

FIG. 2. Crystalline structure of the orthorhombic Te-III phase. The structure consists of puckered layers parallel to the x-z plane, and has four atoms per unit cell. The layers are stacked along the y direction and alternatively shifted by half a lattice constant along the x direction. Each atom has four intralayer first nearest neighbors at distances d_{1-2}, d_{1-3}, and $d_{1-4} = d_{1-5}$, and four interlayer second nearest neighbors at distances $d_{1-6} = d_{1-8}$ and $d_{1-7} = d_{1-9}$. The dashed lines show the rhombohedral unit cell, which is obtained when the intralayer and interlayer distances are equal.

sure dependence of the different crystal structures, we calculated their total energy (E) as a function of volume (V). For each phase $E(V)$ was obtained by fitting a Murnaghan equation to our calculated energies. The resulting curves are shown in Fig. 3; the various crystal structures can be classified in order of increasing minimum energy as follows: trigonal, sc, rhombohedral, orthorhombic, and bcc.

The trigonal structure has the lowest energy, and is therefore the most stable phase at zero pressure, in agreement with experiment. In our calculation, the rhombohedral structure (Te-IV) has a lower minimum energy than the orthorhombic structure (Te-III), whereas experimentally the orthorhombic phase transforms to the rhombohedral phase under pressure. Both of these structures are metallic, but they have different bonding properties. In particular, Te-III has strong covalent bonds, whereas the close-packed structure of Te-IV is characteristic of a simple metal. The comparison of the total energies of two such structures is delicate since energy differences

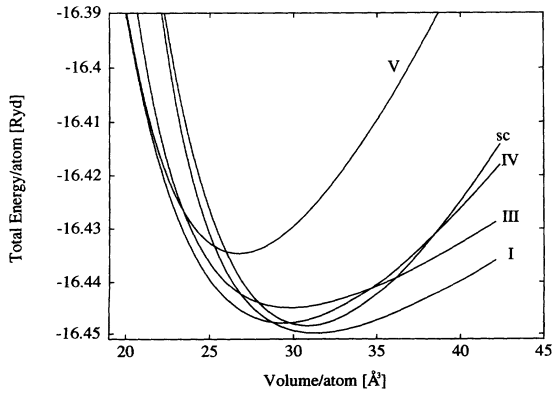

FIG. 3. Total energy per atom as a function of volume for the different crystalline phases of tellurium. The curves are Murnaghan fits to computed values.

as small as 2 mRy/atom are involved. These are of the order of the LDA accuracy. In addition, for such small energy differences phonons energies may become important in determining the relative stability of the structures. The same is true when comparing the trigonal and the sc structures.

In order to assess the accuracy of the pseudopotential approximation in predicting energy differences between the different phases, we have compared the results of the pseudopotential calculations with those of all-electron computations, performed with the FLAPW method. The all-electron calculations have been undertaken for the five structures in their equilibrium configuration, as determined from the pseudopotential calculations. The total energy of the various phases relative to the trigonal phase are (in mRy/atom) 1.4 (sc), 2 (Te-IV), 5 (Te-III), 15 (bcc) in the pseudopotential calculations, and ~0.4 (sc), 2 (Te-IV), 5 (Te-III), 13 (bcc) in the FLAPW calculations, respectively. Even though the energy differences are not identical, the order of the different phases is the same in both calculations. In particular, the minimum energy of the orthorhombic structure is higher than that of the rhombohedral structure. We note that the rhombohedral-orthorhombic structure ordering remains unaltered when using a larger plane-wave energy cutoff or when improving the BZ sampling, in our PW pseudopotential calculations. These results clearly indicate that the discrepancy with experiment in predicting the relative order of Te-III and Te-IV is due neither to the pseudopotential approximation nor to input parameters such as the energy cutoff or the number of k points. As will be discussed in detail in the next section, we believe that the discrepancy is related to the difficulty of the LDA in correctly describing weak bonds, such as those present between the planes of the Te-III structure.

In Fig. 4 we compare the volume as a function of pressure, $V(P)$, as obtained from the Murnaghan equations of state, with the corresponding experimental results. For Te-I to Te-IV, the theoretical trends of $V(P)$ are

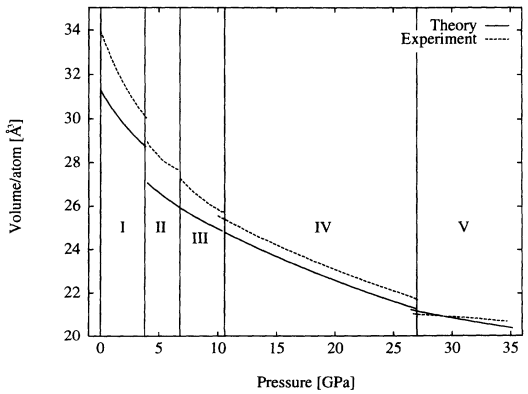

FIG. 4. Calculated (solid line) and experimental (dashed line) (Ref. 3) equation of state for the different crystalline phases of tellurium. The theoretical curve of the orthorhombic Te-III phase has been extended to lower pressures where the monoclinic Te-II phase is actually observed.

in good agreement with experiment, except for the standard LDA volume underestimation. The error in the volume, however, is larger for the trigonal and orthorhombic phases than for the rhombohedral phase, for which theory and experiment agree very well over the whole pressure range. As far as the $V(P)$ curve for Te-V is concerned, the agreement between theory and experiment is not very good. We will discuss this point in detail in the next section.

From the fitted equations of state, one can easily compute the volume, the bulk modulus (B), and its pressure derivative (B'), at any given pressure. In Table I, we listed for comparison the theoretical and experimental results for these parameters at given pressures selected in the experimental study.[3] The calculated volumes for both the rhombohedral and the bcc structure are in good agreement with experiment, whereas those for the trigonal and the orthorhombic phases are underestimated by 4–5 %. As far as the bulk moduli are concerned, there are substantial discrepancies between calculated and measured values. The large discrepancy for the bulk modulus of Te-V will be analyzed in Sec. IV D, together with the discussion of $V(P)$. It is noteworthy that in the experiment only a small range of volumes was accessible, which makes the fitting procedure difficult, in particular at very high pressures.

IV. BONDING PROPERTIES UNDER PRESSURE

A. Trigonal phase (Te-I)

In Table II, the calculated lattice constants and internal parameters of Te-I at equilibrium and at 3.8 GPa are listed, and compared with experiment. The lattice constants are in satisfactory agreement with the measured values.[38] The error for a (3.8%) is much larger than for c (0.7%) thus leading to an unusually large error for the equilibrium volume. Our calculated values for the first and second nearest-neighbor distances show similar differences. The first nearest-neighbor distance d_1 is overestimated by 2.5%, whereas the second nearest-neighbor distance d_2 is 5.4% too small.

These differences reflect the anisotropic character of the trigonal structure (see Fig. 1), and emphasize the distinct nature of intra- and interchain bonding. The underestimation of the lattice constant a and especially of d_2 is larger than that found by LDA calculations in covalent materials. The LDA significantly underestimates (7%) the interchain equilibrium distance, which is indeed controlled by interactions weaker than those of typical covalent bonds. As a consequence of the underestimation of d_2, the nearest-neighbor distance d_1 is slightly overestimated by our calculations.

The pressure dependence of d_1 and d_2 and of the lattice parameters are shown in Figs. 5(a) and 5(b), respectively. Comparison with the experimental results show that our calculated curves correctly reproduce the trends under pressure (see also Table II), and in particular the highly anisotropic behavior of the structural parameters. The lattice parameter c and the intra-chain distance d_1 barely change with increasing pressure, whereas pressure induces a strong decrease in both a and d_2. Hence the structure of the chains is only slightly affected when the pressure is increased. The decrease in volume under pressure is mainly due to the large decrease in a. These results highlight the distinct character of intra- and interchain interactions. The former are strong and directional, characteristic of covalent bonding, whereas the latter are much weaker, allowing the chains to be easily pushed together at low pressure. Roughly speaking, at low pressure the trigonal structure can be seen as composed of weakly interacting rigid one-dimensional units.

Even if the behavior of the lattice parameters as a function of pressure is correct, the pressure derivatives at low P are underestimated by our calculations, especially for a and d_1. The experimental curve has a large slope at low P, the interaction of atoms on neighboring chains being weak. When the pressure increases, the slope diminishes, reflecting the increasing repulsion between adjacent chains. Since our calculation predicts too small a second neighbor distance—therefore overestimating the magnitude of the interchain interaction—the large change in a and d_1 at low pressure cannot be reproduced. At higher P the discrepancies between the experimental and calculated values of a and d_1 are smaller. The errors in a and c are comparable, indicating that as the interaction between chains becomes stronger, the distinct nature of intra- and interchain bonding found at low P tends to vanish.

In Fig. 6 we show the band structure of Te-I at equilibrium. One can clearly identify bands triplets. By using a molecular-orbital picture, these can be interpreted as arising from s bonding (-14 to -8 eV), p bonding (-6 to

TABLE I. Calculated and experimental volumes per atom (V_r), bulk moduli (B_r), and pressure derivatives of the bulk moduli (B'_r) for the different crystalline phases of Te at some reference pressures P_r. The experimental data from Ref. 3 are given in parentheses.

Phase	P_r [GPa]	V_r [Å^3]	B_r [GPa]	B'_r
I	2.0	29.8	47.3	7.0
		(31.3)	(24)	(2.3)
III	8.5	25.0	71.6	6.0
		(26.2)	(57)	(4.0)
IV	17.5	23.1	113.7	4.1
		(23.6)	(115)	(2.0)
V	33.0	20.5	216.0	4.5
		(20.6)	(425)	(5.0)

TABLE II. Structural parameters of the trigonal phase, Te-I, at equilibrium and at 3.8 GPa. Experimental values from Ref. 38 are given in parentheses. Distances are in Å and angles in degrees.

Pressure	a	c	d_1	d_2	θ	u
0 GPa	4.28	5.89	2.90	3.30	100.9	0.287
	(4.45)	(5.93)	(2.83)	(3.49)	(103.32)	(0.263)
3.8 GPa	4.11	5.90	2.90	3.18	101.1	0.300
	(4.19)	(5.98)	(2.81)	(3.33)	(104.74)	(0.273)

-3 eV), and p lone-pair (-3 to 0 eV) and p antibonding states (0 to 3 eV), respectively. The antibonding states form the lowest conduction band. The p bonding and the p lone-pair states can be related to intra- and interchain bonding, respectively. Some characteristic energy differences of the band structure are reported in Table III, where they are compared with experiment. It is seen that the calculated direct gap at H is very small. However, it is remarkable that our calculation *does* predict a gap for the trigonal phase of Te, since the LDA gap underestimation is typically larger than $\sim$0.5 eV. We also note that the lowest unoccupied band at A lies very close to the Fermi level. Our calculated value of the indirect H-A gap is smaller than that found by earlier calculations, which were performed at the experimental values of the structural parameters, and thus at a value of c/a smaller than that obtained after optimizing the crystal structure.

Except for the underestimated energy gaps, our calculated band structure is consistent with experiment. As a consequence of the overestimation of the interchain bonding we expect the band dispersion to be slightly too large. If the band structure had been calculated at the experimental c and a values, with the chains further apart, the dispersion would have been smaller, as has recently been observed for selenium.[24] The large band dispersion in Fig. 6 explains why a large number of k points is required in order to obtain a good convergence of the total energy.

Before discussing the phases of Te under pressure, it is useful to compare the equilibrium structure of Te with that of other VIa elements. At equilibrium, Se has the same structure as Te, but a larger d_2/d_1: 1.43, to be compared with 1.23 in Te. Therefore, the model of a highly anisotropic solid built of one-dimensional weakly interacting units is more justified for Se than for Te. Nevertheless this picture was useful in discussing the properties of the trigonal Te-I phase under pressure. Polonium has a simple cubic structure at equilibrium (α-Po) and a rhombohedral structure (β-Po) under pressure.[39,40] Both of these structures can be simply related to the Te trigonal structure. The β-Po rhombohedral phase is obtained for the special value of the internal parameter $u = 1/3$, which leads to $d_2/d_1 = 1$; with the further condition $c/a = \sqrt{3/2}$ the sc structure of α-Po is obtained (see Fig. 1). According to these simple relationships, one could expect the trigonal structure of Te to directly transform to the sixfold coordinated rhombohedral structure under pressure. Reality is more complex. The trigonal structure first transforms into a slightly monoclinic structure (Te-II), then into an orthorhombic structure (Te-III), and finally into a phase with the rhombohedral structure (Te-IV).

B. Orthorhombic phase (Te-III)

The identification of the Te-II and Te-III structures has been the subject of controversy[41–44] for some time.

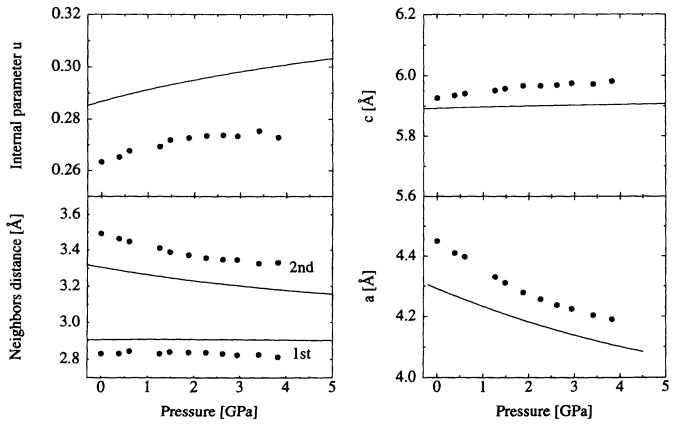

FIG. 5. Pressure dependence of the structural parameters of the trigonal Te-I phase. Internal parameter u and nearest-neighbor distances d_1 and d_2 (left-hand side panel), lattice parameters a and c (right-hand side panel). The solid lines are the calculated results and the points are from experiment (Ref. 38).

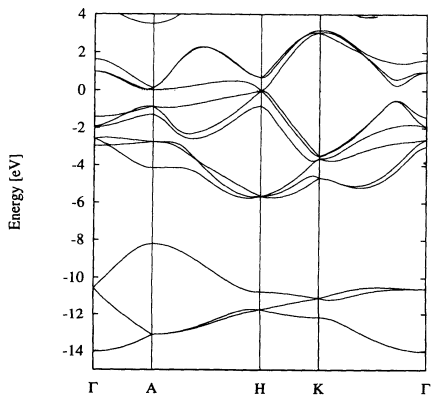

FIG. 6. Band structure of the trigonal Te-I phase. One can clearly identify bands triplets arising from s (-14 to -8 eV), p bonding (-6 to -3 eV), p lone pair (-3 to 0 eV), and p antibonding states (0 to 3 eV).

TABLE III. Characteristic energy differences of the band structure of the trigonal phase, Te-I, at equilibrium, together with the corresponding experimental values. Energies are in eV.

	LDA	Expt.
Direct gap at H	0.02	0.33[a]
Direct gap at A	0.8	
Width of the lowest valence band	5.8	~ 6[b]
Width of the upper valence band	5.7	~ 5[b]

[a] Reference 51.
[b] Reference 52.

Finally these phases were identified by Aoki *et al.*[45] (Fig. 2), who also reported a determination of the internal parameters of Te-II. To our knowledge, the data of Ref. 45 are the only ones for the internal parameters of the two structures. Te-II and Te-III are almost identical: Te-II is monoclinic with an angle slightly different from 90° ($\beta = 92.7°$ at 4.5 GPa), while Te-III is orthorhombic ($\beta = 90°$).[3,45] Even though a small change in volume is observed at the Te-II to Te-III transition, both phases have very similar properties.[45]

Therefore, and in order to reduce the computational effort, we only considered the Te-III phase in our calculations. We believe that our results for the orthorhombic structure in the pressure range of Te-II should also be representative of the monoclinic phase. Thus we regard our calculated lattice and internal parameters, shown in Table IV, as in satisfactory agreement with the experimental data. Intralayer first neighbor distances are overestimated (the maximum error being 5%) for bonds belonging to chains parallel to the c axis (d_{1-2},d_{1-3}), whereas they are underestimated (3%) for bonds parallel to the a axis ($d_{1-4} = a$). Second neighbor distances between layers (d_{1-6}, d_{1-7}) are underestimated (up to 2%).

Experimental data show that with increasing pressure the lattice constants a and c change little, whereas b decreases significantly.[45] This behavior is confirmed by our calculations. The comparison of the internal parameters for different volumes (Table IV) shows that the effect of the pressure is mainly to decrease the interlayer distance. This indicates that strong covalent-type of bonds exist within the layers, despite the metallic character of Te-III, and furthermore that the bonding between layers is weak. Similarly to Te-I, the structure of Te-III (and Te-II) can be described as being built of rigid low-dimensional units, in this case two-dimensional planes, weakly interacting with each others. However, the intra- to interplane distance ratio is smaller than the intra- to interchain distance ratio in Te-I, and the distinction between strong and weak bonds in the layered structure of Te-III is not as clear as in Te-I. It is nevertheless noticeable from the pressure-induced changes in the lattice parameters.

The similarity between Te-I and Te-III can help us understanding why at equilibrium the energy differences between the orthorhombic and the rhombohedral structure of Te-IV is not reproduced correctly (see Sec. III) by our calculation. We saw that in the trigonal structure the anomalous volume underestimation is mainly due to the LDA failure to correctly describe the weak interchain bonding. Similarly the length of weak bonds, i.e., the intralayer distance of Te-III, is underestimated by the LDA. We believe that the failure of LDA to properly account for some of the bonding properties of Te-III is responsible for the incorrect energy ordering between Te-III and Te-IV. We note that similar difficulties of the LDA to describe weak bonds are found for other elements with a layered structure, such as the group-Va elements arsenic,[46] antimony, and bismuth, and more extremely the graphite form of carbon.

The picture of Te-III as being built of two-dimensional rigid layers allows us to understand the mechanism of the Te-III to Te-IV transition, in which a fourfold coordinated, anisotropic, planar-type structure transforms to a sixfold coordinated three-dimensional structure. We saw that the effect of increasing pressure is to reduce the interlayer distance, thus eventually reaching the configuration in which the interlayer and intralayer distances will be equal. If we furthermore assume that the first, second, and third neighbor distances are all equal, the resulting structure can easily be identified as being the rhombohedral lattice of Te-IV.

C. Rhombohedral phase (Te-IV)

Te-IV has the β-Po-like rhombohedral structure with only one atom per unit cell. The structural parameters are the lattice constant a_r and the angle α_r between the unit cell vectors; they correspond to the distance between

TABLE IV. Structural parameters of the orthorhombic phase, Te-III, at 4.5 GPa and 9 GPa. For a definition of the symbols, see Fig. 2. The experimental results (Ref. 45) given in parentheses are for the monoclinic structure ($\beta = 92.71°$) at 4.5 GPa. Distances are in Å and angles in degrees.

Pressure	$a = d_{1-4}$	b/a	c/a	d_{1-2}	d_{1-3}	d_{1-6}	d_{1-7}	θ_{2-1-3}	θ_{2-1-4}
4.5 GPa	3.02	2.37	1.64	2.80	3.25	3.43	3.45	110	90
	(3.10)	(2.42)	(1.54)	(2.80)	(3.10)	(3.47)	(3.52)	(107.9)	(87.3)
9 GPa	3.00	2.29	1.61	2.98	2.97	3.29	3.35	109	90

TABLE V. Structural parameters of the rhombohedral phase, Te-IV, at 11.5 GPa and at 27 GPa. The experimental results from Ref. 42 are given in parentheses. Distances are in Å and angles in degrees.

Pressure	$d_1 = a_r$	d_2	α
11.5 GPa	3.01	3.74	103.0
	(3.00)	(3.72)	(103.3)
27.0 GPa	2.94	3.54	109.3

the six nearest neighbors and to their bond angle, respectively. The Te-IV structure can also be described as a trigonal structure (Te-I type) with three atoms per unit cell. In Table V we report the calculated lattice parameters of the rhombohedral structure at 11.5 GPa and at 27 GPa, i.e., near the transition pressure to Te-V, together with the experimental data at 11.5 GPa.[42] The agreement with experiment is excellent.

In Fig. 7 the energy variations of the rhombohedral structure as a function of α_r, $E(\alpha_r)$, is plotted for different volumes, corresponding to pressures ranging from 0 to 30 GPa. All of these curves show two minima: one at $\alpha < 90°$ and the other at $\alpha > 90°$. The latter has always the lowest energy, and corresponds to the experimentally observed structure. From these curves we can easily see how the rhombohedral structure transforms to the bcc structure of Te-V: α_r slowly increases as pressure increases up to about 27 GPa, where it reaches a value of 109.28°; this value yields the bcc structure. Since the Te-IV to Te-V phase transition is of first order, the two local minima in $E(\alpha)$, for $\alpha > 90°$, are expected to be separated by a small energy barrier. The first minimum should occur at α_r and the second at $\alpha = 109.28°$. However, the small energy variations between 100° and 110° and the very small change in volume observed during the rhombohedral-bcc transition makes the calculation of the energy barrier beyond the accuracy of our calculation.

The structure that corresponds to the local minimum for $\alpha < 90°$ has never been observed experimentally; it is interesting to note that it could be obtained from the trigonal structure of Te-I when $u \to 1/3$. When relaxing the trigonal structure, we found that for large values of c/a the internal parameter u indeed relaxed to 1/3. This may be related to the metallic character of the trigonal structure for c/a ratios larger than the equilibrium one. The simple cubic structure is another special case of the rhombohedral structure when $\alpha = 90°$. All of the $E(\alpha)$ curves for volumes smaller than the equilibrium volume exhibit a maximum at 90°. This indicates that the simple cubic structure is unstable at any positive pressure, and that it cannot be observed experimentally.[21,42]

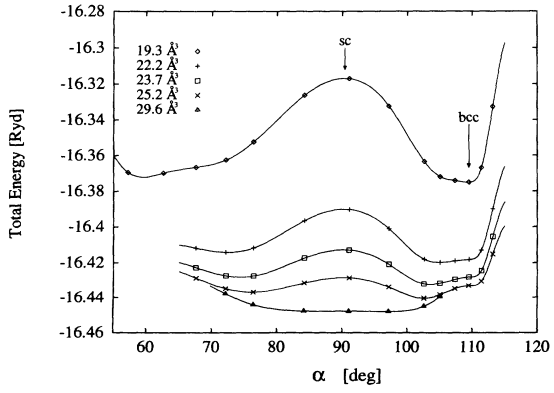

FIG. 7. Total energy of the rhombohedral Te-IV structure as a function of the unit cell angle α. The different volumes correspond to effective pressures up to 50 GPa.

D. Body-centered-cubic phase (Te-V)

In Sec. III we saw that the calculated and experimental curves $V(P)$ did not agree very well for the bcc structure. The experimental bulk modulus was considerably larger than the theoretical one. We performed extensive tests to investigate the origin of this discrepancy. We first improved the BZ sampling, and then increased the plane-wave cutoff in our pseudopotential calculations. Neither a large increase in the number of k points (up to 250 special k points) nor the use of the tetrahedron interpolation method for the BZ integration had any significant effect. The same conclusion applies to the use of large energy cutoffs (up to 36 Ry). We then tested the influence of the chosen pseudopotential, by generating a new one according to the Troullier-Martins[47] prescription, and by including the f contribution to the nonlocal part. Their influence was again found to be negligible.

Finally we performed all-electron FLAPW calculations, thus taking core relaxation effects into account. We also carried out FLAPW calculations with the 4d electrons treated as valence states, which did not alter our previous conclusions in any manner. It could be argued that the LDA itself is responsible for the observed discrepancy with experiment, since both the FLAPW and the pseudopotential calculations rely on that approximation. However, the excellent results found for the rhombohedral phase, which is very similar to the bcc structure, indicates that this is rather unlikely. The bcc structure is a special case of the rhombohedral structure, and we do not expect any dramatic change in the properties of the crystal at the phase transition, and a sudden breakdown of our approximations.

We note that for pressures below ~30 GPa, the experimental volumes of the bcc phase are smaller than the LDA computed volumes. This is at variance with the great majority of LDA results: Volumes are almost *always* underestimated in LDA calculations, which is indeed the case for all of the phases studied here, but for the bcc. Furthermore, we note that for the other group-

VIa element Se, the rhombohedral to bcc phase transition is only weakly first order, which is consistent with our finding for tellurium. To our knowledge there has been so far only one x-ray diffraction study of the Te-IV↔Te-V transition.[3] For other pressure-induced transitions in tellurium and selenium there has been much controversy[4,6] concerning the measured volume discontinuity at the transitions. We therefore think that further experimental studies of this transition would help settling the issue of the occurrence of a relatively large discontinuity for the bcc phase in the equation of state of solid Te.

V. CONCLUSIONS

We have investigated the relative stability and the pressure dependence of various Te polymorphs by means of first-principles local-density calculations. To our knowledge, this is the first *ab initio* study of solid Te under pressure. Only very recently computational techniques have been developed with the accuracy and speed necessary for these type of calculations. Our results for the structural trends of the different phases under pressure show good general agreement with experiment. Furthermore, our calculations account for the pressure dependence of the trigonal and orthorhombic structures, which can be explained, respectively, in terms of chains and planes moving almost rigidly under pressure.

Excellent agreement between the calculated and experimental structural parameters was obtained for the compact high-pressure rhombohedral phase. For the trigonal equilibrium phase, the calculations systematically underestimate the interchain second neighbor distances, and therefore overestimate the intrachain first neighbor distances. Such trends are characteristic of the LDA for open structures which include weak bonds. Similar differences are found for the intra- and interlayer distances in the high-pressure orthorhombic phase. These changes in the Te bond lengths are relatively small, since they do not exceed 6% in either phases.

However, since LDA tends to underestimate the binding energy of structures in which weak bonds are present, the predictions are not in full agreement with the experimental relative stability of the phases under pressure. In particular, the LDA calculations fail to predict the transition from the orthorhombic to the rhombohedral structure under pressure. For similar reasons, we find the twofold coordinated trigonal equilibrium structure to be only 0.1 eV/atom lower in energy than the sixfold coordinated simple cubic structure. In this connection, we note that recent simulations[48] of liquid Te performed within the LDA predicted a sixfold coordinated state, in contrast with the experimental evidence of a threefold coordination in the liquid. We believe that the low estimate of the energy difference between the trigonal and simple cubic phase as predicted by LDA explains the difficulties encountered in simulating the liquid.

There has been some effort to go beyond the LDA by including gradient corrections in the calculation of the Te trigonal structure.[49,50] Although the ratio between intra- and interchain distances improved with such corrections, an opposite trend was observed for other structural parameters. Such calculations also yielded a bulk modulus in poor agreement with experiment. There is thus no definitive answer yet to the LDA problem for open structures. Further effort in this area is still needed.

ACKNOWLEDGMENTS

It is a pleasure to thank A. Baldereschi and R. Car for useful discussions. This work was supported by the Swiss National Science Foundation under Grant No. 20-39528.93. Computations were performed at the CSCS in Manno.

* Present address: Physics Department, Keele University, Keele, Staffordshire ST5 5BG, United Kingdom.

[1] See, e.g., review articles in MRS Bull. **18**, No. 5 (1993); *High Pressure Science and Technology*, edited by S. C. Schmidt, J. W. Shaner, and M. Ross (American Institute of Physics, Woodbury, NY, 1993).
[2] H. K. Mao and R. J. Hemley, Rev. Mod. Phys. **66**, 671 (1994).
[3] G. Parthasarathy and W. B. Holzapfel, Phys. Rev. B **37**, 8499 (1988).
[4] G. Parthasarathy and W. B. Holzapfel, Phys. Rev. B **38**, 10105 (1988).
[5] N. Cuo, R. G. Greene, and Arthur L. Ruoff, Phys. Rev. Lett. **71**, 2943 (1993).
[6] Y. Akahama, M. Kobayashi, and H. Kawamura, Phys. Rev. B **47**, 20 (1993).
[7] J. Fortner, M. L. Saboungi, and J. E. Enderby, Phys. Rev. Lett. **69**, 1415 (1992).
[8] J. E. Enderby and A. C. Barnes, Rep. Prog. Phys. **53**, 85 (1990).
[9] R. Biswas, R. M. Martin, R. J. Needs, and O. H. Nielsen, Phys. Rev. B **30**, 3210 (1984); **35**, 9559 (1987); M. T. Yin and M. L. Cohen, Phys. Rev. Lett. **50**, 2006 (1983).
[10] M. T. Yin and M. L. Cohen, Phys. Rev. B **26**, 3259 (1982); **26**, 5668 (1982).
[11] B. H. Cheong and K. J. Chang, Phys. Rev. B **44**, 4103 (1991).
[12] N. E. Christensen and M. Methfessel, Phys. Rev. B **48**, 5797 (1993).
[13] N. Binggeli and J. R. Chelikowsky, Nature **353**, 344 (1991); J. R. Chelikowsky, H. E. King, Jr., N. Troullier, J. L. Martins, and J. Glinnemann, Phys. Rev. Lett. **65**, 3312 (1990).
[14] C. Nice, Y. Lu, and C. Lieber, Science **261**, 334 (1993).
[15] H. C. Hsueh, J. Crain, S. J. Clark, and G. J. Ackland (unpublished).
[16] J. D. Johannopoulos, M. Schlüter, and M. L. Cohen, Phys.

Rev. B **11**, 2186 (1975).
[17] *Gmelin Handbook of Inorganic Chemistry, Tellurium*, edited by G. Czack, D. Koschel, and H. H. Kugier (Springer-Verlag, Berlin, 1983), Suppl. Vol. A2, pp. 107–110.
[18] T. Starkloff and J. D. Joannopoulos, J. Chem. Phys. **68**, 579 (1978).
[19] H. Isomäki, J. von Boehm, P. Krusius, and T. Stubb, Phys. Rev. B **22**, 2945 (1980).
[20] L. R. Newkirk and C. C. Tsuei, Phys. Rev. B **4**, 2321 (1971).
[21] C. Weigel, R. P. Messmer, and J. W. Corbett, Phys. Status Solidi B **57**, 455 (1973).
[22] G. Doerre and J. D. Joannopoulos, Phys. Rev. Lett. **43**, 1040 (1979).
[23] D. Vanderbilt and J. D. Joannopoulos, Phys. Rev. **27**, 6296 (1983).
[24] H. Akbarzadeh, S. J. Clark, and G. J. Ackland, J. Phys. Condens. Matter **5**, 8065 (1993).
[25] J. Ihm, A. Zunger, and M. L. Cohen, J. Phys. C **12**, 4409 (1979); **13**, 3095 (1980).
[26] H. J. F. Jansen and A. J. Freeman, Phys. Rev. B **30**, 561 (1984).
[27] D. M. Ceperley and B. J. Alder, Phys. Rev. Lett. **45**, 566 (1980).
[28] J. P. Perdew and A. Zunger, Phys. Rev. B **23**, 5048 (1981).
[29] L. Hedin and B. I. Lundqvist, J. Phys. C **4**, 2064 (1971).
[30] R. Stumpf, X. Gonze, and M. Scheffler (unpublished).
[31] C. G. Broyen, Math. Comput. **19**, 577 (1965).
[32] S. Froyen, Phys. Rev. B **39**, 3168 (1989).
[33] H. J. Monkhorst and J. D. Pack, Phys. Rev. B **13**, 5188 (1976).
[34] C. L. Fu and K. M. Ho, Phys. Rev. B **28**, 5480 (1983). As far as quantum-mechanical forces are concerned, the terms relative to the single orbital contributions are simply weighted by the electronic level occupation number. This procedure ensures a proper variational scheme for total energies computed with the Gaussian broadening technique.
[35] W. C. Davidon, Math. Programm. **9**, 1 (1975).
[36] G. Lehmann and M. Taut, Phys. Status Solidi B **54**, 469 (1972).
[37] V. V. Brazhkin, R. N. Voloshin, S. V. Popova, and A. G. Umnov, J. Phys. Condens. Matter **4**, 1419 (1992).
[38] R. Keller, W. B. Holzapfel, and H. Schulz, Phys. Rev. B **16**, 4404 (1977).
[39] A. von Hippel, J. Chem. Phys. **16**, 372 (1948).
[40] J. Donohue, *The Structure of the Elements* (Wiley, New York, 1974), p. 387.
[41] S. S. Kabalinka, L. F. Vereshchangin, and B. M. Shulenin, Zh. Eksp. Teor. Fiz. **45**, 2073 (1963) [Sov. Phys. JETP **18**, 1422 (1964)].
[42] J. C. Jamieson and D. B. McWhan, J. Chem. Phys. **43**, 1149 (1965).
[43] J. Donohue, Z. Kristallogr. **139**, 159 (1974).
[44] See, e.g., Ref. 17, pp. 33–34.
[45] K. Aoki, O. Shimomura, and S. Minomura, J. Phys. Soc. Jpn. **48**, 551 (1980).
[46] R. J. Needs, R. M. Martin, and O. H. Nielsen, Phys. Rev. B **33**, 3778 (1986).
[47] N. Troullier and J. L. Martins, Phys. Rev. B **43**, 1993 (1991).
[48] F. Kirchhoff, Diploma thesis, Ecole Polytechnique Fédérale de Lausanne, 1993.
[49] A. Dal Corso, Ph.D. thesis, International School for Advance Studies, Trieste, 1993.
[50] G. Kresse, J. Furthmüller, and J. Hafner (unpublished).
[51] V. B. Anzin, M. I. Eremets, Yu. V. Kosichkin, A. I. Nadezhdinskii, and A. M. Shirokov, Phys. Status Solidi A **42**, 385 (1977).
[52] M. Schlüter, J. D. Joannopoulos, M. L. Cohen, L. Ley, S. P. Kowalczyk, R. A. Pollak, and D. A. Shirley, Solid State Commun. **15**, 1007 (1974).

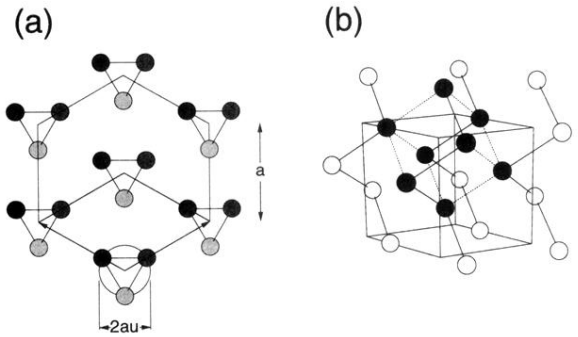

FIG. 1. Crystalline structure of the equilibrium Te-I trigonal phase. Projection of the structure along the c axis (a) and side view (b). The structure is characterized by infinite helical chains with three atoms per turn. The chains are arranged on an hexagonal lattice and are parallel to the c axis. The internal parameter u defines the position of the atoms in the unit cell as $(u,0,0),(0,u,1/3),(\overline{u},\overline{u},2/3)$ in units of the lattice vectors. The radius of the chains is given by au and the interchain distance is $a(1-u)$. The simple cubic structure is a special case of the trigonal structure obtained for $u=1/3$ and $c/a=\sqrt{3/2}$. The cubic framework is indicated by dashed lines.

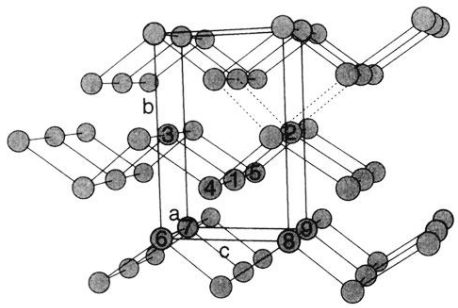

FIG. 2. Crystalline structure of the orthorhombic Te-III phase. The structure consists of puckered layers parallel to the x-z plane, and has four atoms per unit cell. The layers are stacked along the y direction and alternatively shifted by half a lattice constant along the x direction. Each atom has four intralayer first nearest neighbors at distances d_{1-2}, d_{1-3}, and $d_{1-4} = d_{1-5}$, and four interlayer second nearest neighbors at distances $d_{1-6} = d_{1-8}$ and $d_{1-7} = d_{1-9}$. The dashed lines show the rhombohedral unit cell, which is obtained when the intralayer and interlayer distances are equal.